Use of Ion-Assisted Sputtering Technique for Producing Photocatalytic Titanium Dioxide thin films: Influence of Thermal Treatments on Structural and Activity Properties based on the Decomposition of Stearic Acid

[6] V.Vishnyakov, [3] P.J. Kelly, [4] J. Humblot, [5] R.J. Kriek, [2] N. S. Allen, [1] N. Mahdjoub

[1] *CRECHE, Center for Research in Environmental Coastal Hydrological Engineering, School of Engineering, University of KwazuluNatal, Durban, South Africa*

[2] *School of Science and the Environment, Faculty of Science and Engineering, Manchester Metropolitan University, Chester Street, Manchester M1 5GD, UK*

[3] *Surface Engineering Group, Faculty of Science and Engineering, Manchester Metropolitan University, Chester Street, Manchester M1 5GD, UK*

[4] *Department of Energetic,INSA de Lyon, FRANCE*

[5] *Electrochemistry for Energy & Environment Group, Research Focus Area: Chemical Resource Beneficiation (CRB), North-West University, Private Bag X6001, Potchefstroom 2520, South Africa*

[6] *Department of Engineering and Technology, Electron Microscopy and Materials Analysis, School of Computing and Engineering, University of Huddersfield, Huddersfield, HD1 3DH, UK*

E-mails: Corresponding author norman_allen@sky.com
Authors contact: V.Vishnyakov@hud.ac.uk, Peter.Kelly@mmu.ac.uk, cobus.kriek@nwu.ac.za, jphc.humblot@gmail.com, drnlmahdjoub@gmail.com

Keywords: titanium dioxide, ion sputtering deposition, photocatalysis, anatase, rutile, mixed phases, temperature treatment

Abstract

Titanium dioxide thin films were deposited by the reactive ion-assisted sputtering method from titanium targets at various partial pressures and deposition parameters. The films were deposited onto substrates at temperatures ranging from room-temperature conditions to 722 K. A selection of thin films was post-deposited annealed at temperatures up to 972 K for 10 minutes and characterized by micro-Raman spectroscopy and scanning electron microscopy (SEM) and subsequently analysed to assess their photocatalytic activity. Micro-Raman characterization revealed that the as-deposited films had either predominant amorphous, rutile-like structures, anatase-like structures or anatase-rutile mixed structures. The thin films deposited with a high substrate temperature and with energy assistance from the ion source tended to be amorphous, while films deposited on a hot substrate without ion energy assistance tended to have a mixed crystalline phase. On subsequent annealing the amorphous films changed to a rutile structure at temperatures above 672 K, while mixed anatase-rutile films changed to predominant rutile structures only after thermal treatments above 872 K. Thus, this study has revealed an astonishing persistence of the anatase-rutile mixed phase at very high temperatures and showed the possible existence of a key transition temperature at 672 K, where it was possible to see a transformation from amorphous or mixed phase to a rutile or dominant rutile mixed phase. Photocatalytic tests were undertaken by using a novel method consisting of observing the degradation of a film of stearic acid by the thin films under artificial UV radiation. Of the films investigated those with anatase-rutile mixed phases showed the greatest photoactivity. This work was essential in the understanding of the correlation between growth deposition conditions, phase transitions and photocatalytic activity. This set of experiments demonstrated that titania made under a highly oxidizing atmosphere, with no temperature applied on the substrate during fabrication and using an ion sputtering method, is a useful and valuable novel method for creating active TiO_2 thin films.

1. Introduction

There is an increasing interest in extending functional film properties. With properties such as high refractive index, wide band gap and chemical stability, TiO_2 can be used in a large range of applications [1-3]. Furthermore, TiO_2 can be deposited on a variety of substrates, such as glass slides, silica glass, silver, porcelain bricks, metal panels, etc. The resulting coatings possess great potential for various industrial applications, including photocatalytic surfaces [4-5].
As one of the most important wide-band-gap (Energy >3 eV) oxides, titania has been extensively academically studied and technologically researched for decades. The electrochemical properties of titanium dioxide are applied to photovoltaic solar cells and gas sensors. Because of its high dielectric constant, hardness, and transparency, TiO_2 thin films are usable for storage capacitors in integrated electronics, protective coatings, and optical components [6-7].

Numerous key applications of titania are strongly related to the structure and optical properties of TiO_2. TiO_2 is known to have different crystalline forms; anatase, rutile and brookite. Films having dense structure are usually used for solar cell applications while porous films are used for gas sensors. The rutile phase is known to be the most thermodynamically stable phase and has a high

refractive index which makes it the most appropriate for protective coatings [8]. The anatase phase is more reactive with ultraviolet light; therefore, it is used for photocatalysis [9-12]. Amorphous, TiO_2 films are used in biomedical fields by reason of its blood compatibility [13].

TiO_2 thin films and indeed powders have been and are fabricated by different methods for numerous applications [14-29]. It is well known that TiO_2 can exist in a number of crystalline forms with differing physical properties and that the choice of the deposition process has a significant impact on the structure of the film. Generally, TiO_2 films change from amorphous to anatase and then rutile depending on the temperature of calcination. Indeed reports suggest that the structural and optical properties are strongly related to the temperature of calcination[14]. Ion-assisted deposition of materials can produce coatings with improved properties since the ion-assistance can provide incident atoms with additional energy. This added energy can modify the nucleation process, improve film adhesion, increase film density, stimulate mixing of alloy materials to form metastable compounds, trigger phase changes, influence film stress and change film microstructure [15-30]. All these factors can be utilized to modify the optical and physical properties of a coating [15].

In the fabrication of visible light responsive thin films, for example, by sintering and impregnation with solutions of modifiers SEM images showed the formation of compact layers of titanium dioxide with particles of diameter within 15–30 nm. The photocatalytic activity of these synthesized films was demonstrated in the reaction of terephthalic acid oxidation to 2-hydroxyterephthalic acid, proving photogeneration of hydroxyl radicals upon visible light irradiation ($\lambda > 400$ nm). In our work films of titania are produced by magnetron sputtering followed by activation optimisation by thermal treatment and photoreactivity with thin coatings of deposited stearic acid. Other work in our group produced titanium dioxide coatings with silver nanoparticles prepared by sol–gel and reactive magnetron sputtering methods with photoactivity being monitored through the decomposition of bisphenol-A [24].

The anti-microbial photoactivity of nano-anatase particles has been thoroughly investigated in both sol-gel and polymeric films [25]. Particle size and layer thickness were crucial parameters. In our recent work [26] and others [29] photoactivity studies on polymorphs of titanium dioxide show mixed phases with brookite having the highest activity. Thermal pre-treatment with temperature playing a critical role. Fe loading in the TiO_2 lattice as another example, with Fe_2O_3/TiO_2 has been found to be 0.27% at a calcination temperature of 600°C, and irradiation time of 600 min. Here photoactivity was found to be 98.26% of phenol in water undergoing decomposition [27]. Silver doped titania films have also been prepared by magnetron sputtering for antimicrobial activity [28] while in another pressure conditions are important as well as film thickness for the decomposition of methylene blue dye [30]. In this work although many conditions are important we have concentrated here on post heating effects of the substrate on photoactivity.

In this work a broad investigation of the various parameters and properties of titania thin films made by ion-assisted deposition was undertaken. Films were deposited under different conditions and then post-deposition annealed over a range of temperatures to investigate the recrystallisation of the TiO_2 films. The annealing conditions and parameters of deposition were interrelated to the structure and morphology, and the optical properties to the photocatalytic activity. The first aim of

this study was to optimize the photoactivity through control of the crystalline structure followed by photoactivity through the decomposition rate of a thin applied coating of stearic acid.

2. Experimental

2.1. Thin film deposition parameters

Thin titania (TiO_2) samples were deposited at various partial pressures and deposition parameters onto silicon (Si) wafers from a titanium target by ion-assisted deposition (IAD). This technique was chosen because it allows close control over the substrate temperature and the energy delivered to the growing film by the ion source. It was hoped that this would allow coatings with pure anatase, rutile and mixes phase structures to be produced, which could then be characterized in terms of their photoactivity. The thin films were deposited onto substrates with temperatures ranging from 350 to 720 K, as detailed in Table 1. A schematic of the IAD process is given in Figure 1.

Table 1. Thin film Processing conditions for the deposition of titania samples by ion beam sputtering

Sample	Substrate	Ar Partial Pressure(Pa)	O_2 Partial Pressure(Pa)	T (K) of the substrate holder	Deposition time (Hrs)	Film Thickness(µm)
1	Si	$2.0x10^{-2}$	$0.5x10^{-2}$	722	3	1.3
2	Si	$2.13x10^{-2}$	$0.37x10^{-2}$	722	3	1.3
3	Si	$3.0x10^{-2}$	$0.5x10^{-2}$	722	3	1.3
4	Si	$4.0x10^{-2}$	$0.5x10^{-2}$	350	3	2.2
5	Si	$4.0x10^{-2}$	$0.5x10^{-2}$	722	3	1.3
*6	Si	$1.5x10^{-2}$	$1.0x10^{-2}$	350	3	1.3
7	Si	$1.2x10^{-2}$	$1.3x10^{-2}$	298	3	0.3

*Sample 6 – O_2 ion assist conditions: extra energy added by the use of a second ion gun

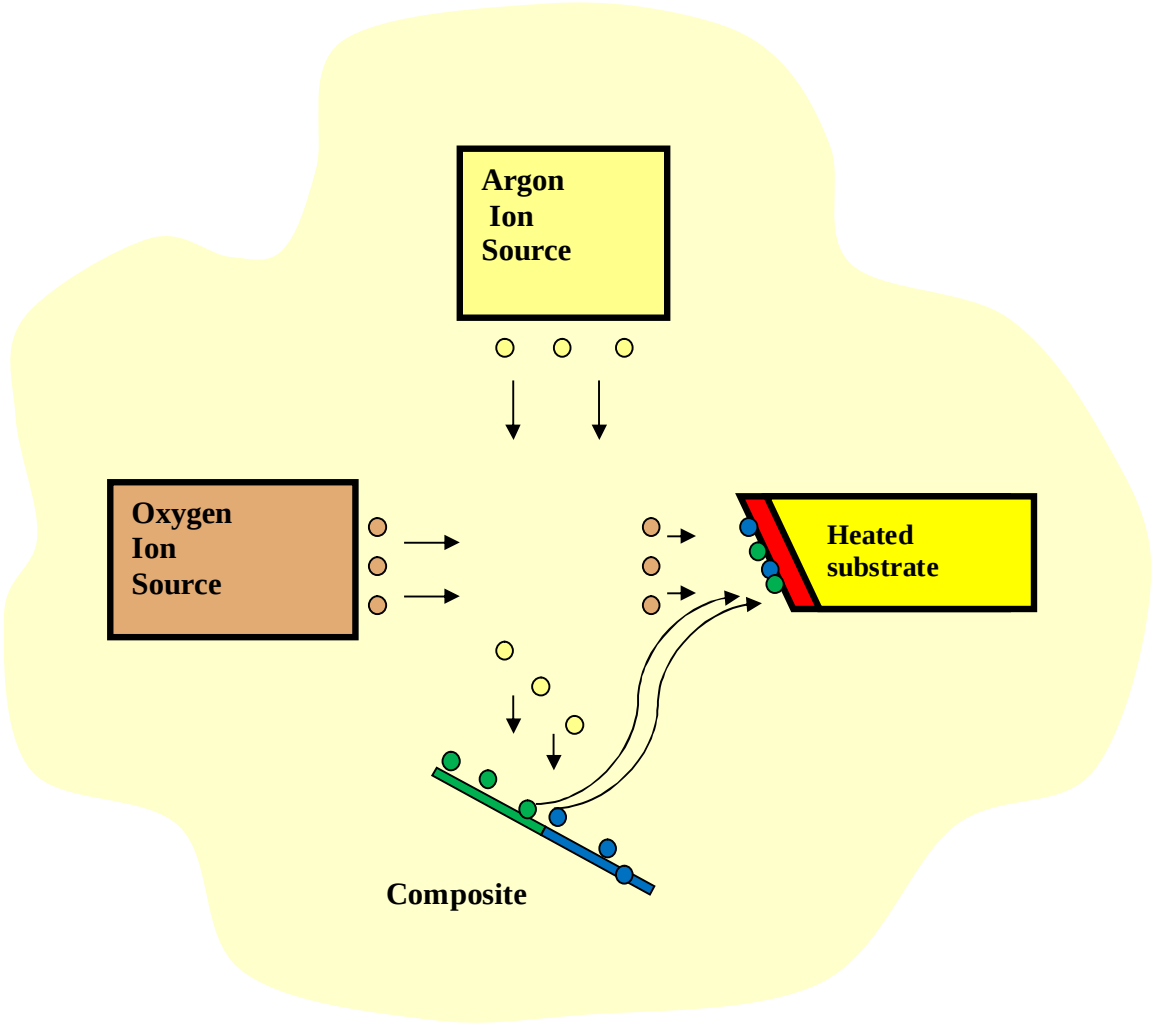
Argon
Ion
Source
Oxygen
Ion
Source
Heated
substrate
Composite

Figure 1. Ion beam IAD system [22]

All the samples were produced by using the main ion gun (Ar) in an oxygen atmosphere. The Ar ion source was used to sputter atoms from an ultra-pure titanium target onto a silicon substrate in an oxygen atmosphere. The atom arrival rate at this substrate was controlled by increasing or decreasing the vertical ion beam current source. Before introducing oxygen into the chamber, a thin 2nm titanium interlayer was deposited onto the silicon substrate. The sputtering pressure was varied in order to assess the effects of a variation of the argon:oxygen flow rate. However, a low flow rate of oxygen has been found to help maintain coating stoichiometry in previous experiments[16] . Only sample 6 was produced with the second assist ion gun (O_2) also in use. The substrate temperature could be independently controlled [2, 17-18]. In order to observe the change in structures and all kinds of phase transformation, the samples were post deposition annealed at temperatures up to 972 K for 10 minutes.

2.2. Material characterization

The TiO_2 samples were examined by micro Raman spectroscopy using an Invia-Microscope from Renishaw. Spectra were taken at 5-6 places and the results were averaged. The spectra were acquired at room temperature with a 514 nm exciting laser. Examples of the spectra obtained are shown in Fig. 2 (a to f).

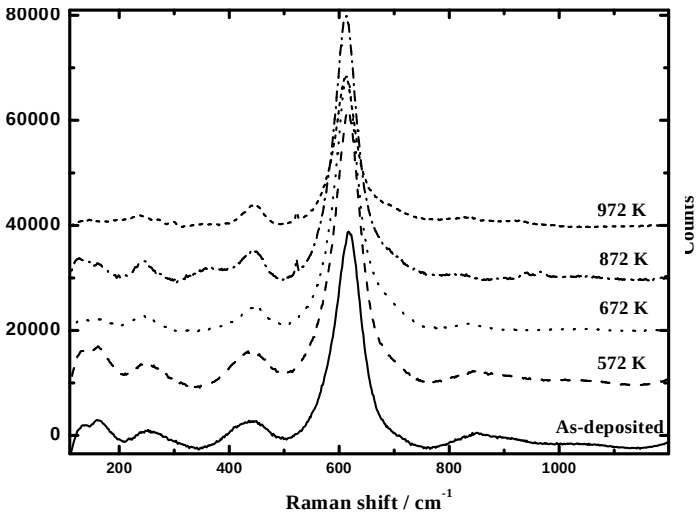

a) Sample 6

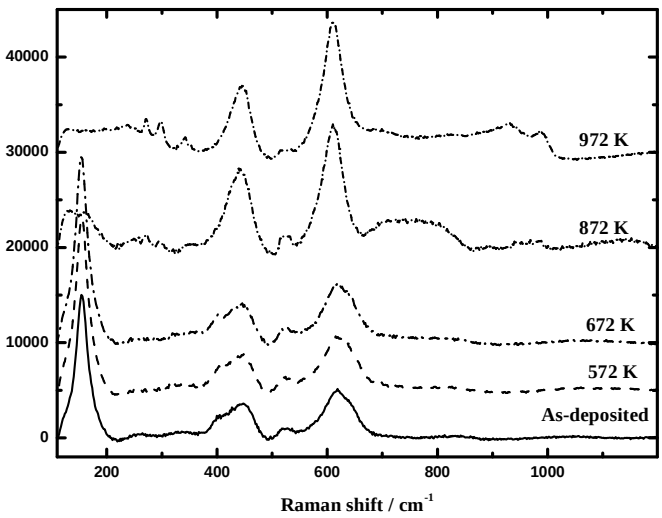

b) Sample 1

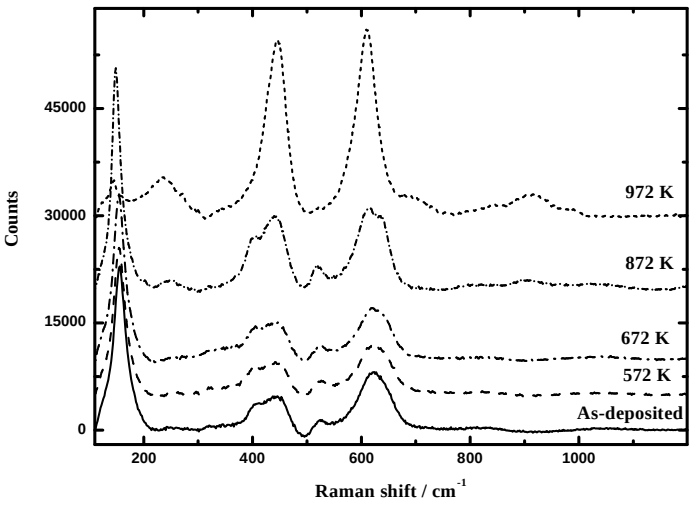

c) Sample 2

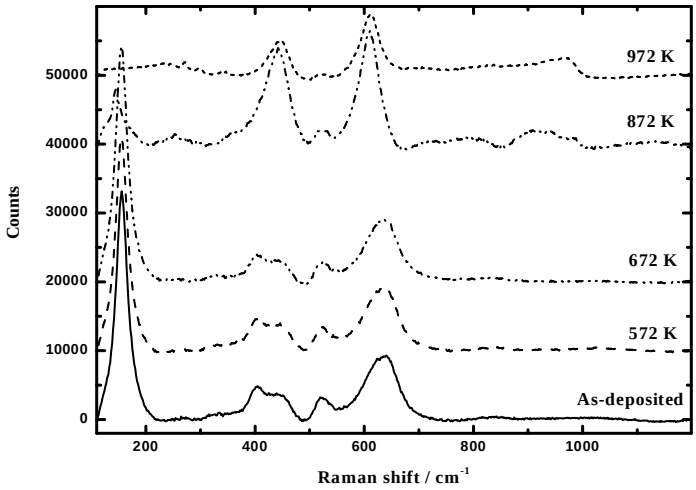

d) Sample 3

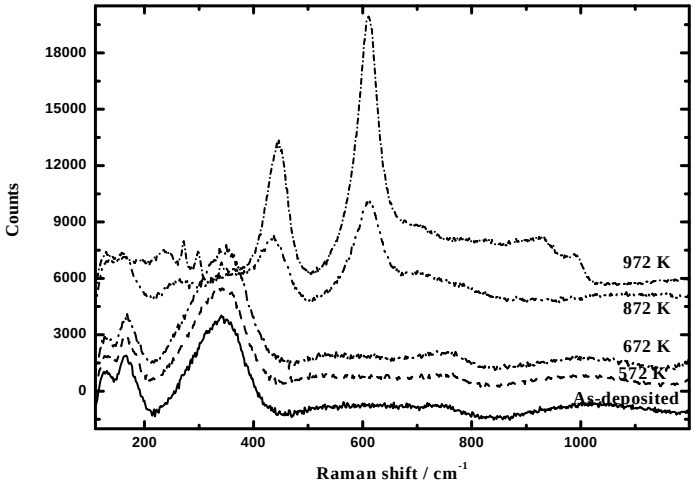

e) Sample 4

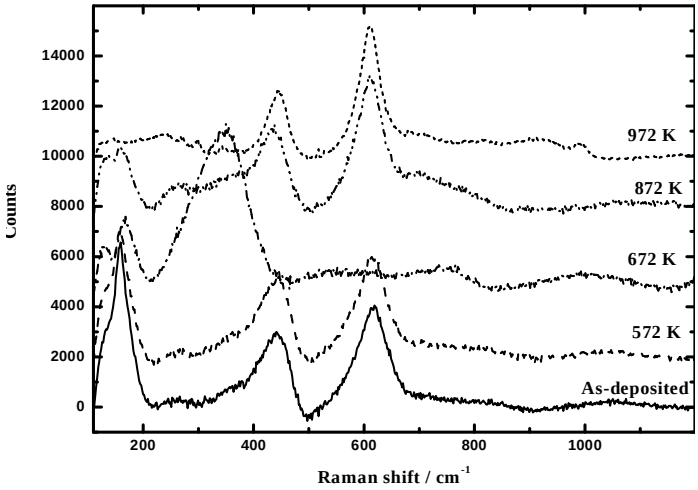

f) Sample 5

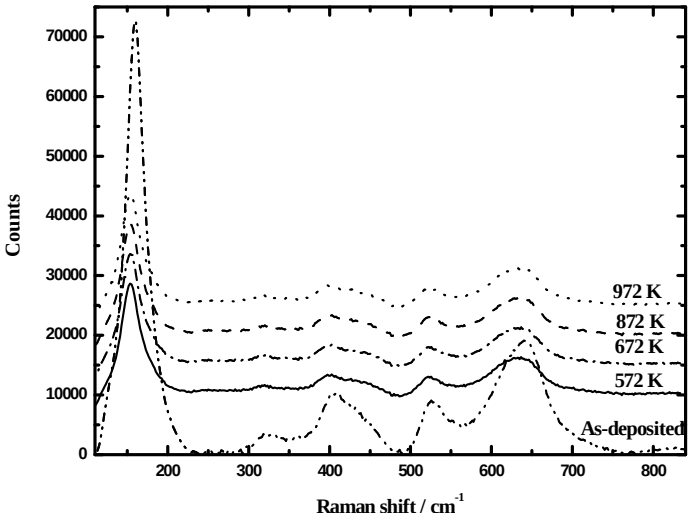

g) Sample 7

Figure 1. Raman spectra of titania coatings deposited at different temperatures and conditions as stated in table 1: a) Sample 6, b) Sample 1, c) Sample 2, d) Sample 3, e) Sample 4, f) Sample 5, g) Sample 7.

The coated substrates were fractured and mounted on Scanning electron microscope (SEM) pin stubs, such that the fracture sections of the coatings could be examined. SEM images of the fracture sections were acquired at room temperature with a Zeiss supra 40 system. The images were made at short working distances (5 to 10 mm) with a small spot size (1.2 nm) in order to obtain a better resolution. The SEM was adjusted so as to minimize the beam penetration, which can increase resolution and surface information. SEM images were taken with a standard aperture (30 µm) so that it's possible to have a good depth of the field and a good resolution (figure 3 for sample 2 is shown as typical example)

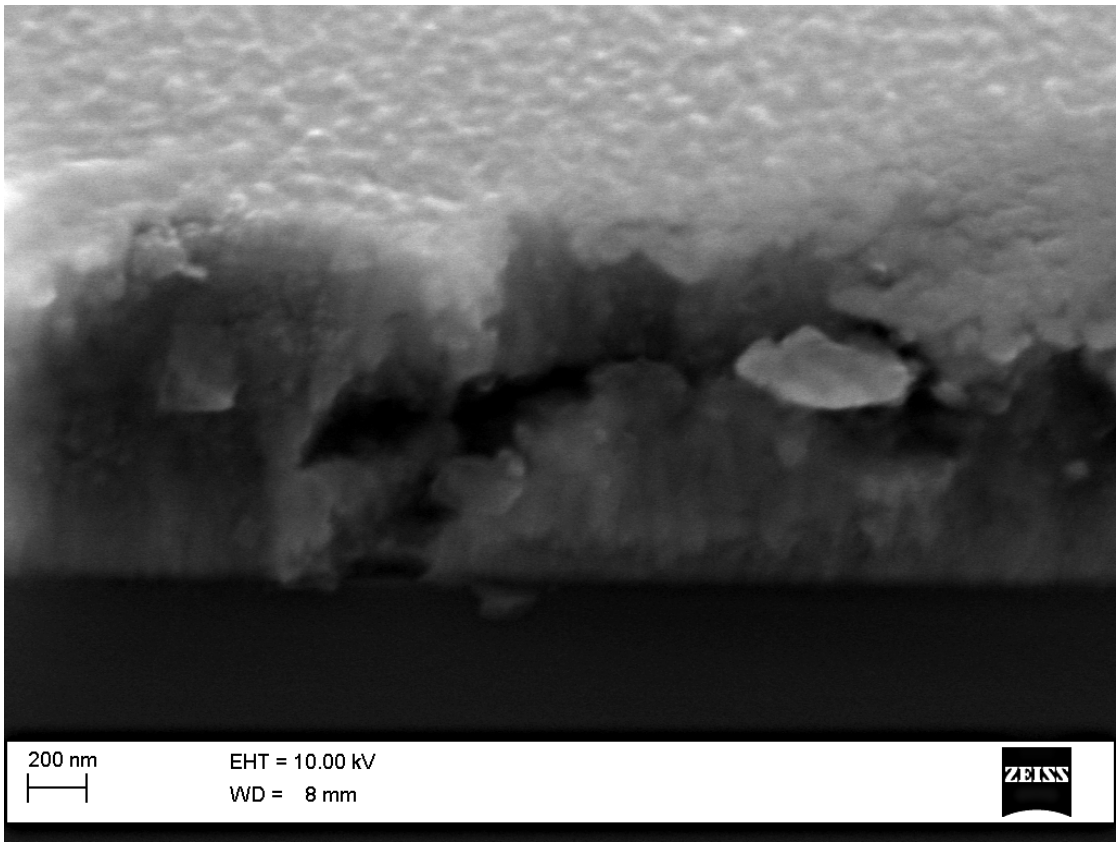

c) Sample 2

Figure 2. Typical SEM micrograph of the samples as-deposited without heat treatments for sample 2 c.

2.3. Photocatalytic test

The level of photocatalytic activity of each film was assessed by observing the degradation of stearic acid exposed to ultra-violet light according to the following method. The sample was first placed in a light box and exposed to 340 nm UV radiation with an intensity of 0.7 W/m^2 for four hours. The sample was then removed and a layer of 10 μl of 10 mmol stearic acid solution in methanol was applied. After that the sample was allowed to dry on top of an oven at 377 K in order to evaporate any residual methanol.

The IR absorption spectrum of the sample was the recorded using a Nicolet Nexus Fourier-transform infrared (FTIR) Spectrometer (DTGS detector). Spectra were recorded at 32 scans with a resolution of $2cm^{-1}$. In order to show the distinctive peaks assigned to the stearic acid (between 2800 and 3050 cm^{-1}), the background was subtracted by analyzing an uncoated stearic acid sample which had been irradiated for the same length of exposure. The measurements were repeated, in order to ensure the methanol was fully evaporated and that the stearic acid was fully crystallized.

The samples were periodically removed from the light box at t= 0, 1h30, 3h30, 7h30 and the IR absorptions were measured. A new background was recorded for each sample and for the same exposure time. Typical examples of the results are shown in Figure 4 (a to e).

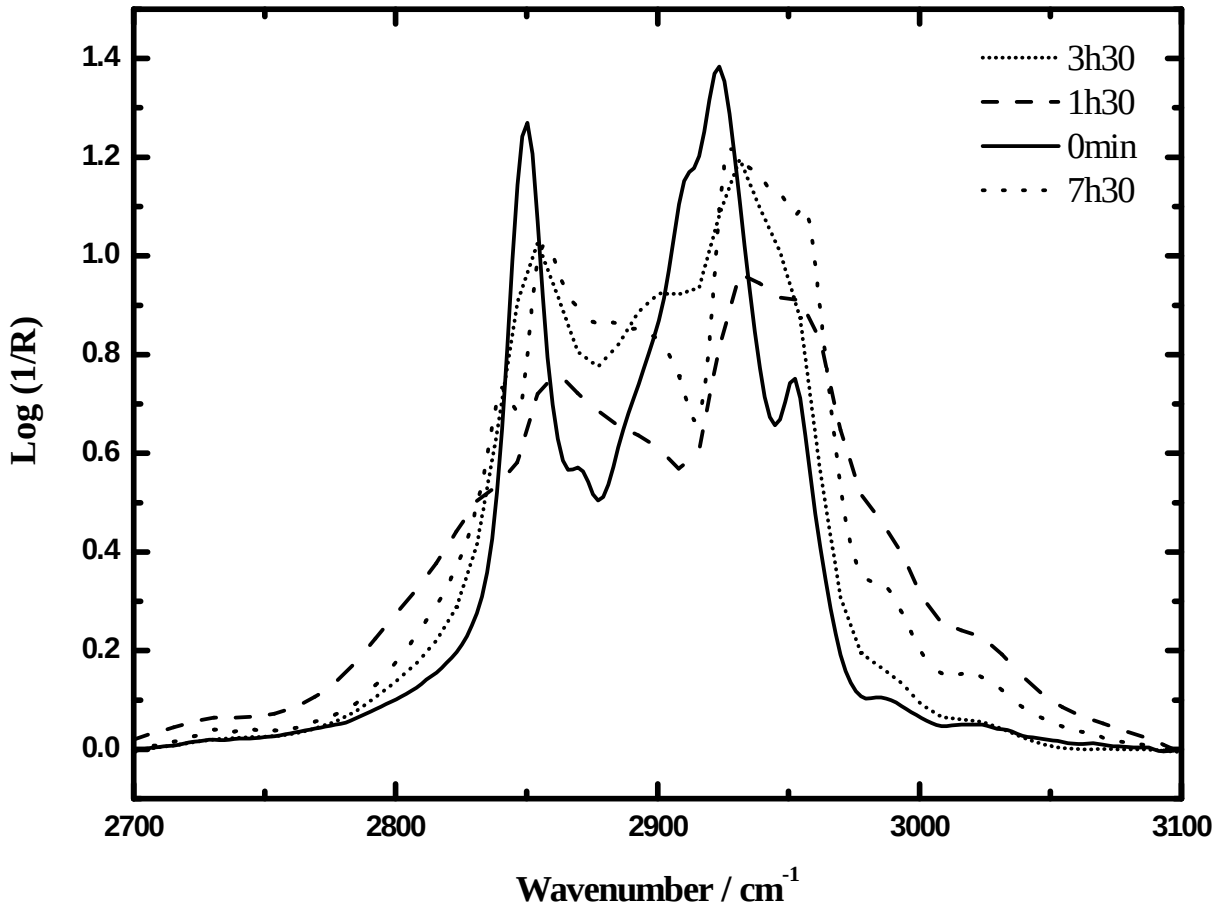

a) RT

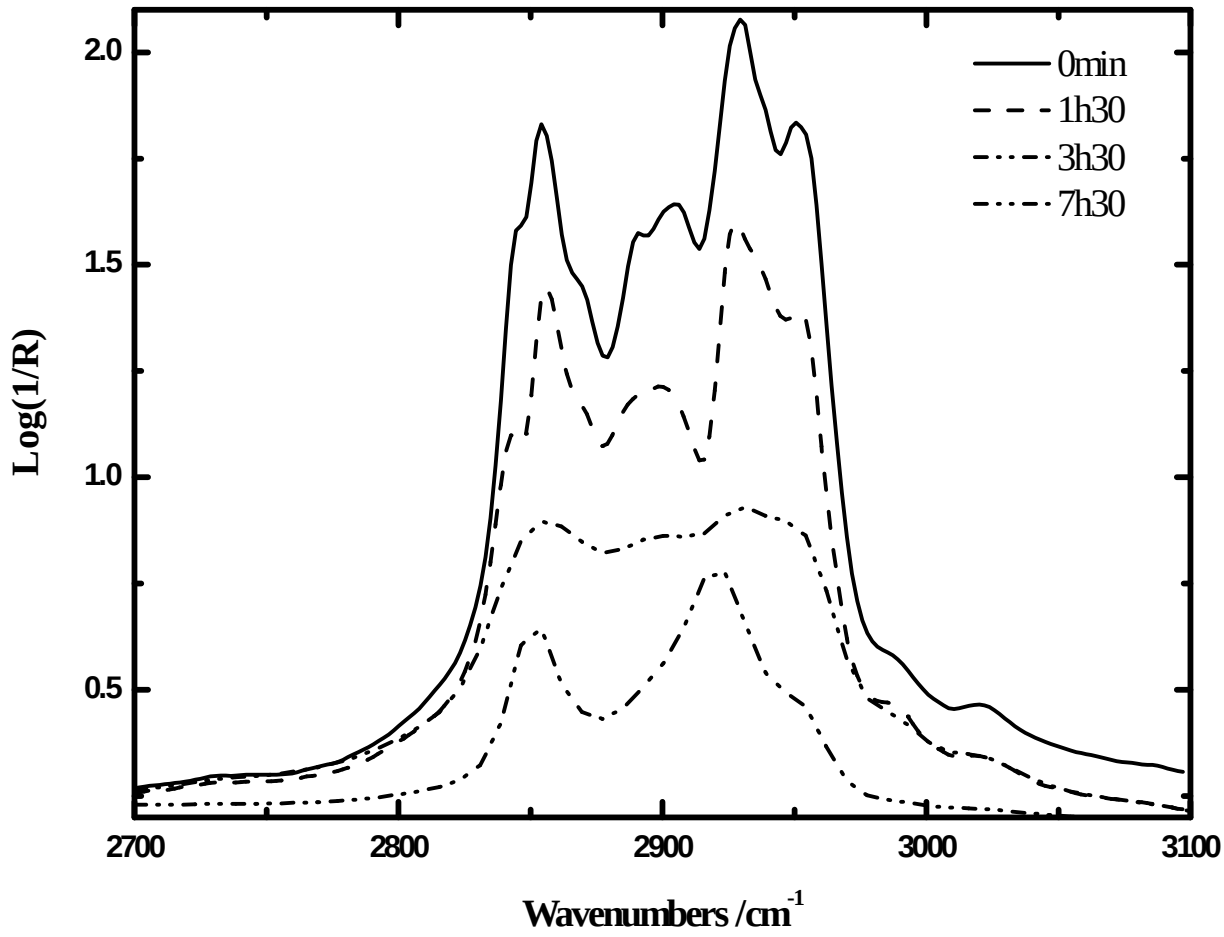
0min
1h30
3h30
7h30
Log(1/R)
2.0
1.5
1.0
0.5
2700
2800
2900
3000
3100
Wavenumbers /cm-1

b) 572 K

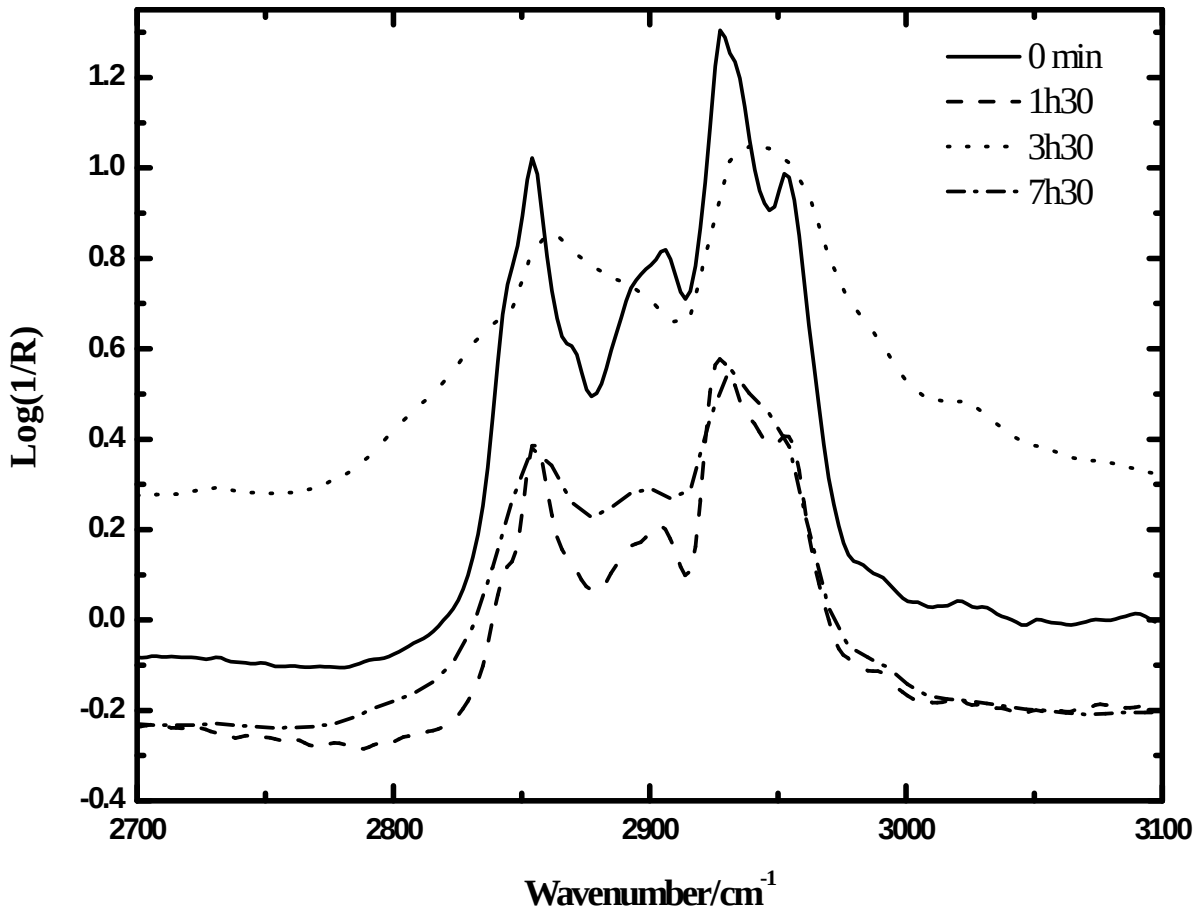
0 min
1h30
3h30
7h30
Log(1/R)
1.2
1.0
0.8
0.6
0.4
0.2
0.0
-0.2
-0.4
2700
2800
2900
3000
3100
Wavenumber/cm-1

c) 672 K

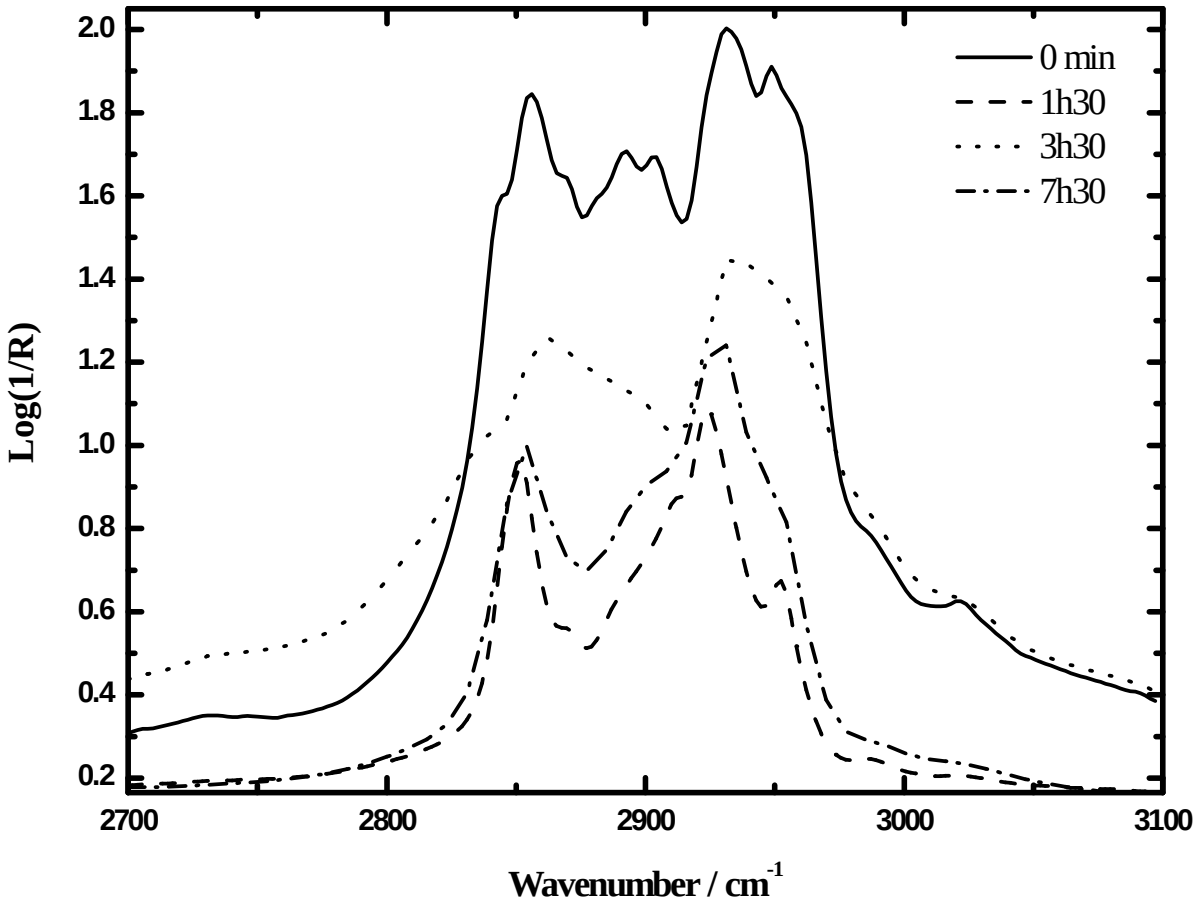
0 min
1h30
3h30
7h30
Log(1/R)
Wavenumber / cm-1
2.0
1.8
1.6
1.4
1.2
1.0
0.8
0.6
0.4
0.2
2700
2800
2900
3000
3100

d) 872 K

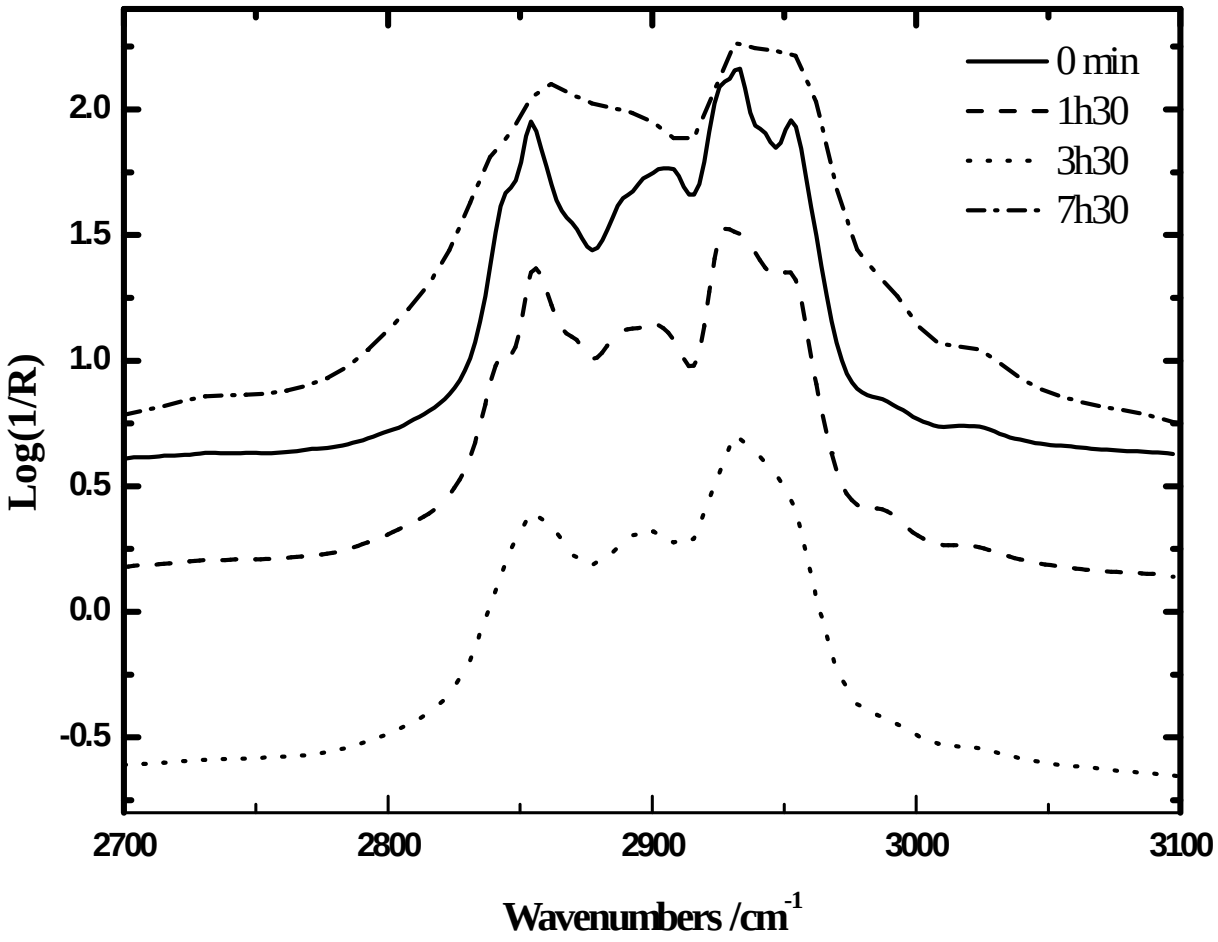

e) 972 K

Figure 3. Photocatalytic assessment of the sample 7 showing reduction in stearic IR bands at a) As-deposited, b) 572K, c) 672K, d) 872K and e) 972K

3. Results and discussion

3.1. Raman analysis

Examples of the Raman spectra obtained for the TiO_2 films are shown in Fig. 2 (a to f) and for convenience the main Raman vibration modes for three titania crystalline phases, taken from

published sources, are summarized in Table 2. All these samples were annealed at temperatures up to 972 K. The annealing conditions, temperature of the substrate holder and the flow rate were modified to change and improve the structure and morphology.

Table 1. Raman peak position/cm-1 for bulk titania phases [19-21].

Brookite	**Anatase**	**Rutile**
128(s)		
135(w)		143(w) B_{1g}
	144(vs) E_g	
153(vs)		
172(sh)		
	197(w) E_g	
214(w)		
235(m) c		
247(m)		
		273(sh)
288(w)		
	320(vs) c	320(w)
322(w)		
		357(w)
366(w)		
396(sh)		
	399(s) B_{1g}	
412(w)		
		447(s) Eg
454(w)		
461(w)		
502(w)		
	515(m) A_{1g}	
		519(m) B_{1g}
545(w)		
585(w)		
		612(s) A_{1g}
636(s)	639(m) E_g	
	695(w) B_{1g}	
		826(w)B_{2g}
		950(sh)

vs, very strong; s, strong; m, medium; w, weak; sh, shoulder band; c, combination.

Samples 1, 2 and 3 were deposited under various Ar and O_2 partial pressures but with Ar being the predominant process gas. These samples had the same temperature applied on the substrate

(722 K). The samples had mixed crystalline phases of anatase and rutile transforming to a rutile-like structure after annealing at 872 K (see figures 2a to c). Samples 4 and 5 were fabricated with the same gas partial pressures; however, the temperature of the substrates during deposition were different. Sample 4 was deposited on a substrate heated at 350 K. This sample (Fig.2e) showed an unusual micro-Raman spectrum which cannot be correlated to any known spectra. The phase remained the same after thermal treatment up to 672 K, while, above 672 K the phase-structure modified and changed to a rutile-like structure which persisted up to 972 K.

Sample 5 was generated on a substrate heated at 722 K. The micro-Raman spectra showed a mixed anatase-rutile phase changing to an unknown phase at 672 K, as observed in sample 5. The structure then changed to rutile-like for annealing temperatures above 672 K. This temperature of treatment appeared to be a crucial temperature in terms of phase determination.

Sample 6 (Fig.2a) was made using a second ion-assist gun bombarding the film with oxygen ions. This added energy was expected to modify the nucleation and growth processes. After analysis, the micro-Raman spectra showed only one peak characteristic of rutile. Although the thin films were annealed, no changes in the phase structure were noticeable. This unusual spectrum cannot be explained at this point.

Sample 7 was the most intriguing sample. This sample had an anatase-rutile structure with a dominance in anatase. The conditions of preparation were unique, with an overall pressure of $2.5x10^{-2}$ Pa and a very high oxidizing atmosphere with an oxygen partial pressure of $1.3x10^{-2}$ Pa. The substrate was not heated and deposition time was 3 hours. In order to assess the phases present, an annealing process was undertaken, which revealed the persistence of this initial as-deposited anatase-rutile like structure up to 972K.

3.2. SEM characterization

All SEM micrographs (see Figure 3 showing sample 2 only as an example) were taken of the as-deposited coatings. Sample 6 was observed to be the most dense due to the extra energy added by the use of a second ion gun. Samples 1, 2 and 3 were similar and had columnar structures with a nano-crystallite feature, the substrate heated at 722 K helped in the growth structure and the thicknesses of both samples were about ~1.3 µm. Sample 4 showed some columnar structure, nano-crystallite growth and was the thickest of the films ~ 2.2 µm. Sample 5 seemed to be formed of interlayers and looked very compact; the thickness was about 1.3 µm. These sample growths were optimized, using different methods; from increasing the temperature of the substrate holder to improving the micro-adhesion to adding extra energy to improve the microstructure and film density.

Finally, sample 7, which was the sample having an anatase/rutile structure remaining unchanged after high thermal treatment, showed a columnar structure with nano-crystallite features. However, the main differences with the other samples came from the thickness and the surface information; due to a high oxidizing atmosphere the sputtering process could not be as efficient as found with the other samples and the absence of applied temperature on the substrate during the fabrication limited the micro-adhesion on the substrate. This sample was found to be very thin, ~0.3 µm, and may be due to oxygen poisoning of the titanium target and covering it with a layer of titania, as

titania sputters at a much lower rate than titanium itself. In the overall picture the structures are broadly similar with 7 being more columnar than the rest of the samples.

3.3. Photocatalytic assessment

Photocatalytic investigations revealed sample 7 to be the uniquely active sample. From Fig.4 showing the IR spectra, sample 7, annealed at 572 K was the most active considering the limited activity of the other samples after a certain exposure time. Fig.5 shows the normalized stearic acid concentration (%) as a function of irradiation time and were obtained by normalising the peak heights in the spectra shown to the zero hour peak. It highlights the activity of the sample annealed at 572 K and reveals an unexpected activity of the sample annealed at 872 K, which also has an anatase-rutile mixed phase structure. All samples annealed at various temperatures are highly active except for the sample investigated as-prepared, which reduces the stearic acid less although it is still active. The initial decay profiles illustrated in figure 5 were fitted to 1^{st} order kinetics, and the 1^{st} order rate constants are given in Table 3. These results were in accordance with the initial statement that sample 7 annealed at 572 K was the most active.

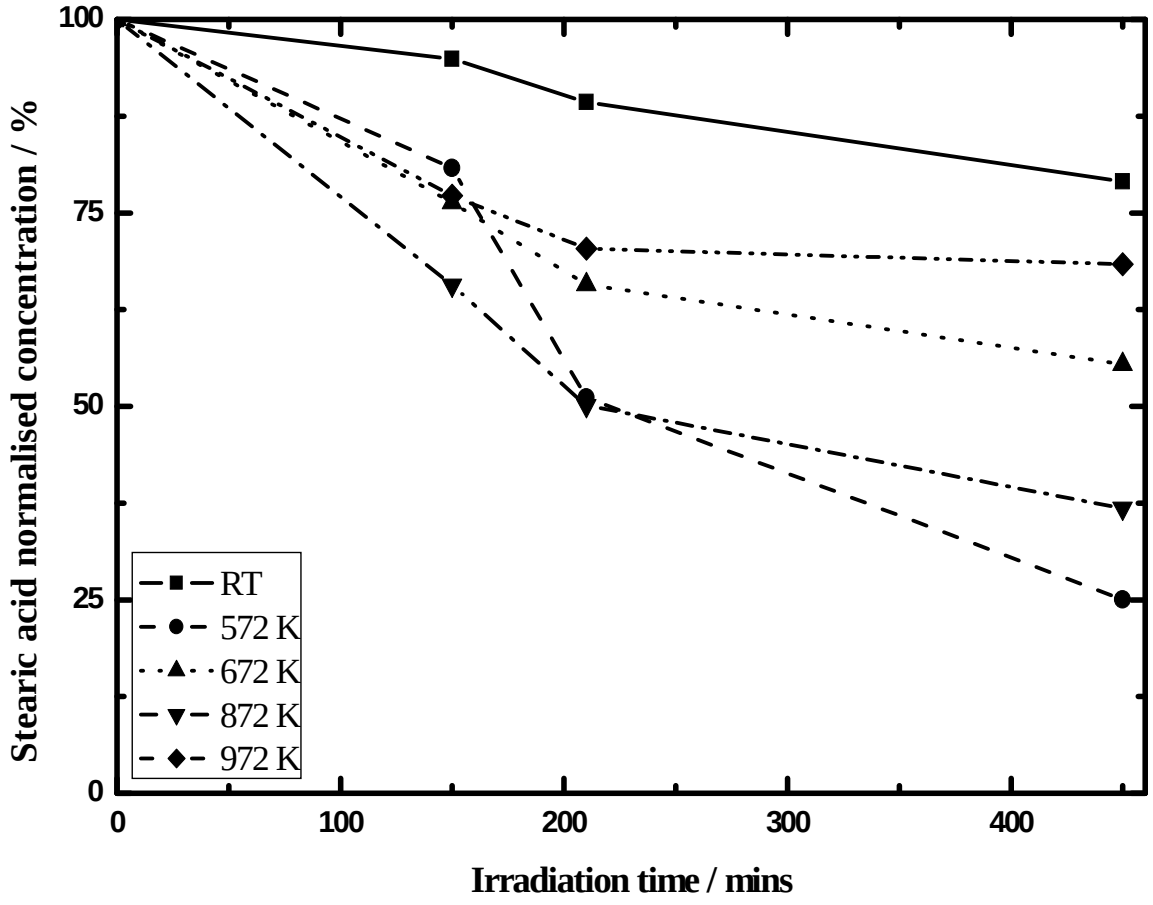

Figure 4. Reduction of absorption at 472 nm for the sample 7 coating with layers of stearic acid.

Table 2. Rate constant k (s^{-1}) of Photocatalytic degradation under UV irradiation of stearic acid by titania coatings deposited by IAD

Sample	As-deposited	Annealed at 572 K	Annealed at 672 K	Annealed at 872 K	Annealed at 972 K
Rate constant k (s^{-1})	1.04×10^{-5}	8.03×10^{-5}	2.8×10^{-5}	4.22×10^{-5}	3.4×10^{-5}

4. Conclusions

This study aimed to shed light on parameters influencing the fabrication of photoactive titania thin films made by an ion sputtering process. Different parameters were taken into account; for instance the argon partial pressure, the oxygen partial pressure, the temperature applied on the substrate during fabrication and addition of extra energy. SEM characterization helped in the assessment of the effect of substrate temperature on the sample and in the assessment of the effect of extra energy added. The samples became thicker and denser with a well-defined columnar structure.

Raman analysis consisted of a quick assessment of the phase in the presence after fabrication and after thermal treatment. It revealed an astonishing persistence of the anatase-rutile mixed phase at very high temperature and showed the possible existence of a key temperature at 672 K as, from amorphous or mixed phase, it was possible to see a transformation to a rutile or dominant rutile mixed phase. Investigated anatase-rutile mixed phases (sample 7) showed the best photoactivity. Despite all the used conditions the process failed to create a pure stable anatase phase during the experiments, however, a mixed phase of anatase-rutile with a dominant anatase phase structure was produced and showed persistence after thermal treatment. This set of experiments exposed the facts that titania made under a highly oxidized atmosphere, with no additional heating applied to the substrate during fabrication, using an ion sputtering method, was a useful and valuable method for creating active TiO_2 thin films (~0.3 μm as-deposited) and with a stable phase structure persisting after thermal treatments up to 972 K. This work like many others such as Fe doping [28] indicate temperature, heating time and phase changes to be critical in controlling photoactivity [17-29].

5. References

1. L.A.Brook, H.A Foster, M.E. Pemble, D.W. Sheel, A. Steele, H.M. Yates. “Study of the Efficiency of Visible-Light Photocatalytic Degradation of Basic Blue Adsorbed on Pure and Doped Mesoporous Titania Films”Surface and Coatings Technology. 201 (2007) 9373-9377.
2. Young Ran Park.” Structural and optical properties of rutile and anatase TiO_2thin films: Effects of Co doping” Thin Solid films. 484 (2005) 34-38.
3. C.J. Tavares, S. Lanceros-Méndez, V. Sencadas, V. Teixeira, J.O. Carneiro,A.J. Martins, A.J. Fernandes. “Strain analysis of photocatalytic TiO2 thin films on polymer substrates” Thin Solid films. 516 (2008) 1434-1438.
4. Bing L.Guo , Zhaolin Hong, Liang Jiang, Huixin, “Sol gel derived photocatalytic porous TiO_2 thin films”, Surface and Coatings Technology. 198 (2005) 24-29.
5. A.Fujishima, T.N. Rao, and D.A. Tryk. “Titanium Dioxide Photocatalysis”, Journal of Photochemistry and Photobiology C: Photochemistry Reviews. 1 (2000) 1-21.
6. Yu, Y., J. Wang, and J.F. Parr, Preparation and properties of TiO2/fumed silica composite photocatalytic materials. Procedia Engineering, (2012), 27(0): p. 448-456.

7. S.A. Chamber, R.F.C.Farrow, R.F.Marks, J.U. Thiele, L.Folks, M.G. Samant, A.J.Kellock, N.Ruzycki, D.L. Ederer and U.Diebold, "Epitaxial growth and properties of ferromagnetic co-doped TiO_2 anatase", Appl. Phys. Lett. 79(2001) 3467.
8. H.M. Takikawa, Takaaki Sakakibara, Tateki Bendavid, Avi Martin, J. Philip, "Properties of titanium oxide film prepared by reactive cathodic vacuum arc deposition", Thin Solid Films. 348(1999) 145-151.
9. J.Yu, X. Zhao, and Q. Zhao., "Effect of surface structure on photocatalytic activity of TiO_2thin films prepared by sol-gel method", Thin Solid Films, 379 (2000) 7-14.
10. J.Yu, X. Zhao, and Q. Zhao, "Photocatalytic activity of nanometer TiO_2 thin films prepared by the sol–gel method", Materials Chemistry and Physics. 69 (2001) 25-29.
11. J.Z.Yu, Xiujian Zhao, Qingnan Wang, Gao, "Preparation and characterization of super-hydrophilic porous TiO_2 coating films", Materials Chemistry and Physics. 68 (2001) 253-259.
12. M.Y.Zhou, Jiaguo Liu, Shengwei Zhai, Pengcheng Jiang, Li, "Effects of calcination temperatures on photocatalytic activity of SnO2/TiO2 composite films prepared by an EPD method", Journal of Hazardous Materials. 154(2008) 1141-1148.
13. Feng Zhang, Ping Yang, Xiaolan Zeng, Yingjun Mao, Zhihing Zheng, Zhuyao Zhou, Xianghuai Liu, "Blood compatibility of titanium oxide prepared by ion-beam-enhanced deposition", Surface and Coatings Technology. 84(1996) 476-479.
14. N.R.M. Mathews, Erik R. Cortés-Jacome, M. A. Toledo Antonio, "TiO_2 Films Influence of Annealing", Solar Energy, Volume 83, Issue 9, September 2009, Pages 1499-1508
15. J.S. Colligon, "Ion-Assisted Sputter-Deposition", The Royal Society, 362(2003) 103-116.
16. P.J. Kelly, Y.Zhou, "Zinc oxide-based transparent conductive oxide films prepared by pulsed magnetron sputtering from powder targets: Process features and film properties", J. Vac. Sci. Technol., 2006. A24 (5): p.1782.
17. P.E.Serpone and Ezio Pelizzetti, Photocatalysis: Fundamentals and Applications. (Wiley, N.Y.) 1989.
18. Q. Ye, Z.F. Tang, L. Zhai, "Hydrophilic properties of nano-TiO_2 thin films deposited by RF magnetron sputtering", Vacuum. 81(2007) 627-631.
19. Ji Guang Li, T. Ishimagaki, " Brookite → rutile phase transformation of TiO_2 studied with monodispersed particles", Acta Materialia. 52(2004) 5143-5150.
20. I.M.S. Arabatzis, T. Bernard, M. C. Labou, D. Neophytides, S. G. Falaras, "Silver-modified titanium dioxide thin films for efficient photodegradation of methyl orange", Applied Catalysis B: Environmental. 42(2003) 187-201.
21. Y.Yu, "Enhancement of photocatalytic activity of mesoporous TiO2 by using carbon nanotubes", Applied Catalysis A: General. 289(2005) 186-196.
22. J.S. Colligon. Nanostructured Thin Films and Nanodispersion Strengthened Coatings. NATO-USSR Advanced Workshop, Springer-Verlag, 30(2004) 297-306.

23. P. Łabuz, R. Sadowski, G. Stochel and W. Macyk, "Visible light photoactive titanium dioxide aqueous colloids and coatings", Chemical Engineering Journal, 230 (2013) 188-194.
24. R. Klaysri, M. Ratova, P. Praserthdam and P. J. Kelly, "Deposition of Visible Light-Active C-Doped Titania Films via Magnetron Sputtering Using CO_2 as a Source of Carbon", Nanomaterials, 7 (2017) 113.
25. L. Caballero, K.A. Whitehead, N.S. Allen and J. Verran, "Photocatalytic inactivation of *Escherichia coli* using doped titanium dioxide under fluorescent irradiation", J. Photochem. & Photobiol., Chem. Ed., 276 (2013) 50.
26. N. S. Allen, N. Mahdjoub, V. Vishnyakov, P. J. Kelly, R. J. Kriek," The effect of crystalline phase (anatase, brookite and rutile) and size on the photocatalytic activity of calcined polymorphic titanium dioxide (TiO2)", Polymer Degradation and Stability, 150, (2018) 31-36.
27. S. Somayeh and A. Farana, "The Effect of FE-Loading and Calcination Temperature on the Activity of FE/TIO_2 in Phenol Degradation", Iran. J. Chem. Chem. Eng., 35, No. 2, (2016) 43.
28. K. Kądzioła, I. Piwońskia, A. Kisielewskaa D. Szczukockib, B. Krawczykb and J. Sielski, "The photoactivity of titanium dioxide coatings with silver nanoparticles prepared by sol–gel and reactive magnetron sputtering methods – comparative studies", Applied Surface Science, 288 (2014), 503.
29. V. Štengla and D. Králová, "Photoactivity of brookite–rutile TiO_2 nanocrystalline mixtures obtained by heat treatment of hydrothermally prepared brookite", Materials Chemistry and Physics, 129 (2011) 794.
30. H. Sabbah, " Effect of sputtering parameters on the self-cleaning properties of amorphous titanium dioxide thin films", J. Coatings Technology and Research, 14 (2017) 1423-1433.